JGR Earth Surface

RESEARCH ARTICLE
10.1029/2024JF007946

Probabilistic Identification of Debris-Flow Pathways in Mountain Fans Within a Stochastic Framework

M. Schiavo[1,2], C. Gregoretti[1], M. Boreggio[1], M. Barbini[1], and M. Bernard[1]

[1]Department of Land, Environment, Agriculture, and Forestry (TESAF), University of Padova, Legnaro (PD), Italy, [2]Department of Geological Sciences, University of Florida, Gainesville, FL, USA

Key Points:

- The probabilistic approach we propose leverages a Monte Carlo framework using an ensemble of synthetic Digital Elevation Models (DEMs) obtained from available DEMs, to identify the most probable debris-flow pathways
- We can assess the probability of an avulsion by validating our approach on field data and consistently using available surveys
- Our approach can be used for predicting future most probable pathways following avulsions based on available DEMs

Supporting Information:

Supporting Information may be found in the online version of this article.

Correspondence to:

M. Schiavo,
massimiliano.schiavo@unipd.it

Citation:

Schiavo, M., Gregoretti, C., Boreggio, M., Barbini, M., & Bernard, M. (2024). Probabilistic identification of debris-flow pathways in mountain fans within a stochastic framework. *Journal of Geophysical Research: Earth Surface*, *129*, e2024JF007946. https://doi.org/10.1029/2024JF007946

Received 31 JUL 2024
Accepted 22 OCT 2024

Author Contributions:

Conceptualization: M. Schiavo
Data curation: C. Gregoretti, M. Boreggio, M. Barbini, M. Bernard
Formal analysis: M. Schiavo, M. Bernard
Funding acquisition: C. Gregoretti
Investigation: M. Schiavo, C. Gregoretti, M. Bernard
Methodology: M. Schiavo, M. Bernard
Project administration: C. Gregoretti
Resources: M. Schiavo, C. Gregoretti, M. Boreggio, M. Bernard
Software: M. Schiavo
Supervision: M. Schiavo, C. Gregoretti

Abstract Debris flows are solid-liquid mixtures originating in the upper part of mountain basins and routing downstream along incised channels. When the channel incises an open fan, the debris flow leaves the active channel and propagates downstream along a new pathway. This phenomenon is called an avulsion. We retrieve the most probable avulsion pathways leveraging a Monte Carlo approach based on using Digital Elevation Models (DEMs). Starting from LiDAR-based DEMs, we build an ensemble of synthetic DEMs using a local Gaussian probability density function of local elevation values and obtain an ensemble of drainage networks using a gravity-driven routing algorithm. The ensemble of drainage networks was used to obtain the most probable pathways of avulsions. We applied our methodology to a real monitored fan in the Dolomites (Northeastern Italian Alps) subjected to debris-flow activity with avulsions. Our approach allows us to verify the consistency between the occurrence probability of a synthetic pathway and those that historically occurred. Furthermore, our approach can be used to predict future debris-flow avulsions, assuming relevance in debris-flow risk assessment and planning of debris-flow control works.

Plain Language Summary Debris flows are impulsive routing of mixtures of water and solid material that start in the upper parts of mountain basins after intense rainfall events. These flows move downstream through channels, carved within the debris fan, which act as preferential pathways. Debris flows can leave original channels and may suddenly change direction and propagate downstream along pathwaysThis phenomenon, called *avulsion*, increases the difficulty for scientists to assess the most probable debris-flow pathways and, much more, future possible ones. We answer this scientific call via a Monte Carlo approach based on an ensemble of synthetic DEMs obtained from available ones. Our framework involves running many simulations, leveraging synthetic possible terrains based on available data, and retrieving as many synthetic equiprobable debris-flow pathway configurations to be wrapped up within a probabilistic framework.

1. Introduction

Debris flows are solid-liquid mixtures of water and sediment that usually occur at the base of cliffs, when abundant runoff delivered by rocky chutes after high-intensity rainfall, impacts debris deposits and, after entraining large quantities of material, forms a surge composed of a solid front and a fluid body (Berti & Simoni, 2005; Gregoretti et al., 2016). The surge routing downstream at high speed erodes the sedimentary bed material, thus forming a solid-liquid current with an increasing magnitude (up to one order of the starting one; Theule et al., 2015). The routing pathway can be divided into high-, intermediate-, and low-sloping. The high- and low-sloping parts of the pathway are dominated by erosion and deposition, respectively, while in the intermediate-sloping reach, erosion and deposition nearly balance themselves (Bernard et al., 2024). Moreover, the route itself can be confined or unconfined. The first case occurs when it runs between two slopes, or when it has a high bed-slope angle ($\geq 20°$ according to Fannin and Wise (2001) and Simoni et al. (2020)) so that erosion processes dominate, and it deeply incises the fan. Conversely, the second case occurs in semi-conical-shaped fans, when the channel-bed slope is not high so that erosion processes do not dominate, and the channel cannot significantly incise the fan. In this case, the deposition of sediments can partially plug or fill the whole cross-section of the channel, hence forcing subsequent flows to take a different pathway on the fan surface, that is, provoking the active channel branching or flow *avulsion* (De Haas, Kruijt, & Densmore, 2018). Avulsions can also result from overtopping in narrow bends when superelevation exceeds the outer banks of the channel (Zubrycky et al., 2021). An avulsion is a process occurring when a debris flow spills out from its active channel, thus concentrating on existing (i.e., paleo) drainage lines or creating new ones, allowing the spatial-temporal evolution of its fan.

Validation: M. Schiavo, M. Bernard
Visualization: M. Schiavo, M. Barbini, M. Bernard
Writing – original draft: M. Schiavo
Writing – review & editing: M. Schiavo, C. Gregoretti, M. Boreggio, M. Barbini, M. Bernard

The phenomenon of avulsion has been approached in the study of fan formation by quasi-cyclic alternations of backfilling, avulsion, and channelization (Hooke, 1967; Van Dijk et al., 2012). De Haas, Kruijt, and Densmore (2018) identified two main causes for the avulsions: the plug of the active channel determined by deposition phenomena occurring for the small inertia of a sequence of small-to moderate-magnitude debris flows, and the levees breaching of a single high-magnitude debris flow. The field investigation of Tsunetaka et al. (2024) confirmed these outcomes. De Haas, Densmore, et al. (2018) analyzed the spatial-temporal evolution of sixteen debris-flow fans all over the world and concluded that: avulsions have a persistent pattern, in the sense that they tend to re-occupy older channels on the fan surface (i.e., inactive or paleo routing pathways). To predict the flow pathways of avulsed flows, de Haas et al. (2019), Zubrycky et al. (2021), and Herbert et al. (2024) analyzed the morphological factors controlling the debris-flow avulsions. De Haas et al. (2019) analyzed nine debris-flow fans in Saline Valley (California) and determined that the channel plug formation is the determinant mechanism for avulsion occurring when the deposition thickness equals or exceeds the channel depth. Zubrycky et al. (2021) examined the spatial impact of debris flows in 146 cases with the results that most avulsions originate at distances between 20% and 40% of the maximum fan length evaluated from the fan apex and their largest fan cross extent is smaller than 40% of the corresponding fan cross extension (i.e., relative to the endpoint of the avulsion). Herbert et al. (2024) studied the relationships between 29 avulsion locations and channel characteristics and determined a site-specific expression in which the avulsion likelihood depends on the percentage of boulders, slope angle, channel width, and the ratio between flow thickness and average slope. Baggio et al. (2024) delineated a framework to improve hazard maps and investigate the impact of various forcings, such as rainfall patterns, on two monitored mountain catchments in the Italian Alps. A method for identifying the flow path of debris-flow avulsions is yet missing. Therefore, we propose a novel methodology to determine all probable debris-flow pathways on sedimentary-shaped fans by a simplified topographic-based approach, relying on both a limited number of available multi-temporal Digital Elevation Models (DEMs) and employing them within a stochastic framework. It is worth noting that in our research, a DEM is intended to be a mathematical representation of the bare earth in digital form (e.g., Vosselman & Maas, 2010), that is, without any overground features (e.g., trees and buildings). The main idea of our research is to move from a limited number of surveyed topographic surfaces toward extrapolating other synthetic surfaces to investigate avulsion directions and spatial patterns in a stochastic way, which is not possible otherwise. Our viewpoint enrolls the multiplicity of information about a fan topography as a "source of uncertainty" that can be exploited to retrieve other possible topographic scenarios. These topographic scenarios, that is, other configurations of the terrain surface, may have existed (but never monitored) in the past, may have happened in the future, or not. But that's not the point: what matters for us is to exploit the widest possible variability of the terrain surface we are working on, upon the available (monitored) DEMs, by generating synthetic digital surfaces. Thus, we consider a Monte Carlo-based approach to infer a set of synthetic digital surfaces for an investigated debris-flow fan. Noteworthy, these approaches are employed in other branches of the hydrological sciences (e.g., Schiavo, 2022, 2023), such as in groundwater flow and transport processes (e.g., Schiavo et al., 2022; Guadagnini et al., 2020, respectively), or landscape evolution processes (e.g., Anand et al., 2023; Bonetti et al., 2020). In the end, merging these approaches allows us to step up in debris flow analysis and assessment by proposing to identify their pathways from a probabilistic perspective leveraging the ability to "create" multiple synthetic (possible, since data-driven) realities.

Developing the ability to represent multiple possible topographic scenarios enables us to analyze the routing network (i.e., the flow patterns) for as many terrain realizations, allowing us to seek any possible spatial variation (read *avulsion*) in flow patterns. For this task, we propose the use of a common routing algorithm (i.e., the "Deterministic-8," also named "D8" flow algorithm; see e.g. Howard, 1990) that, by working along the steepest path, maximizes potential energy losses along the debris-flow route (as e.g. in Orlandini & Moretti, 2009; and aligned with analysis conducted by Pederson et al., 2015). Furthermore, a large enough volume (in the sense of a total volume of Monte Carlo runs, which must be large enough to comply with the numerical stability of the ensemble: see Ballio & Guadagnini, 2004; Schiavo, 2024, as references, as explained in the Methodology) of simulated synthetic routing networks enables us to examine the local probability of a point being routed by a debris flow, hence identifying an avulsion along a certain preferential direction.

Is it possible to employ topographic data time series to probabilistically extrapolate other plausible digital synthetic scenarios of the observed physical reality How possible avulsions can be carved into our domain for many synthetic simulations, hence from synthetic terrain configurations? We aim to answer these questions, as well as the aim to define, if possible, the most probable pathways in the case of avulsions, and to quantify their likelihood

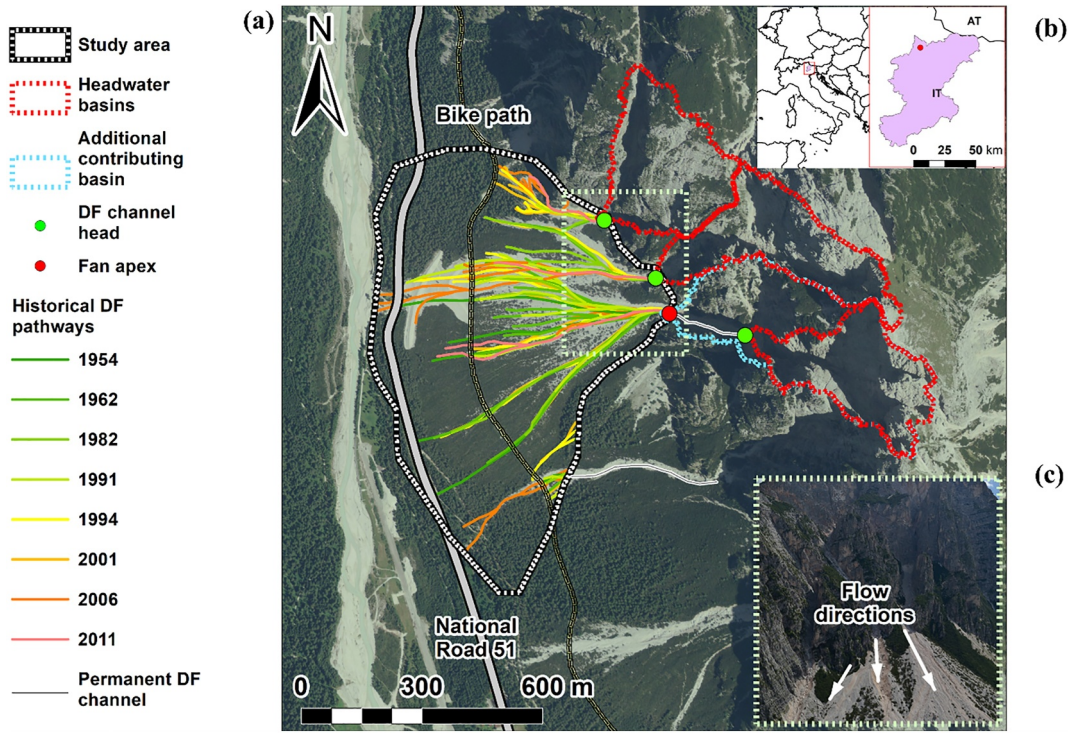

Figure 1. The area of investigation is located in the Belluno province (Northeastern Italy, panel a). Historical debris-flow pathways that occurred from 1954 to 2021 are depicted by colors. Two infrastructures, the National Road 51 and a bike path, overlap in gray and yellow and are located downstream of the debris fan area (within the white polygon), respectively, in panel (b) Panel c illustrates a photo of the two major debris-flow channels downstream of the fan apex, at the feet of the rocky cliff of the *Pomagagnon Ridge*; downslope debris flow preferential directions, following main incised channels, are highlighted by white arrows (panel c).

of occurring. As a result, Our research could represent a valuable source of information for scientists and technicians involved in the study and design of the debris-flow control works. Control works should be positioned for intercepting and conveying the debris flows to an ending retention basin (Barbini et al., 2024). Due to the increased frequency of occurrence of debris flows in the last decades because of the climate transition we are experiencing (Stoffel et al., 2014, 2024), control works are assuming more and more relevance for limiting the socio-economic impact of debris flows (Strouth & McDougall, 2021; Thiene et al., 2017). The expected outcomes of such a framework would be to be able: (a) to provide a simplified and flexible framework to exploit available topographic surveys as much as possible to retrieve information about debris-flow pathways and avulsions; (b) to spatially reproduce the debris-flow pathways and hence potential initiation points (see Gregoretti & Dalla Fontana, 2008) of past and present flows that occurred in a study catchment; these latter points would be identified as the starting locations within the domain where extracted probable pathways stem from. In some cases, the real initiation point's location depends on the morphology of the headwater (upstream) catchment, if any (see e.g. Barbini et al., 2024). Moreover, we aim (c) to provide a quantitative probabilistic assessment of the hazardousness of a domain location to reside onto a possible avulsion, and to seek to predict the best configuration of control works in the case of unconfined debris flows.

2. Methodology

2.1. The Study Area and Historical Data

The National Road SS 51 north to Cortina d'Ampezzo (Dolomites Northeastern Italian Alps, Figure 1, panel a) runs streamwise along the Boite River, following a nearly straight line from km 106 to km 110. This path includes the basis of several debris-flow fans. These fans originate at the base of the rocky cliffs constituting the *Pomagagnon Ridge*. The rocky cliffs are mainly calcareous-dolomitic and belong to the Limestones of the "Calcari Grigi" overlaid by the thick dolomitic succession of the "Dolomia Principale" Formation and are characterized by fractures that make them subject to frequent failures (Marchi et al., 2008). This study is focused on the fan in correspondence of km 109 of SS 51, one of the largest of the considered study areas, which originated

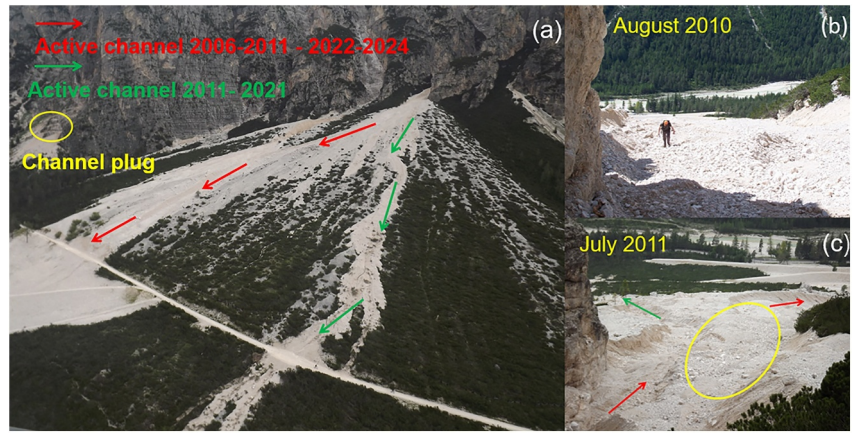

Figure 2. Front view of the investigated debris-flow fan with the shifting of the active channel (a) and two upstream-downstream views of the active channel before (b) and after the shifting (c).

from the deposition of gravely debris via several debris-flow events and cliff failures (i.e., rocky landslides) across the centuries. Here we distinguish a main contributing basin (Gregoretti & Dalla Fontana, 2008), and other smaller basins (see Figure 1, panel b). Gregoretti and Dalla Fontana (2008) determined an initiation area at the base of a cliff where a debris-flow channel starts and initially runs between two straight rocky ridges (Figure 2's panel a, and Figure S1 in Supporting Information S1 panel a) so that the debris flow is continuously supplied by the runoff descending from them. Therefore, Gregoretti and Dalla Fontana (2008) positioned the flow control section at the outlet of the runoff contributing basin area at the apex of the fan where a check-dam as a control structure is located and the rocky ridges end. At the outlet of the other two contributing basins originating at the feet of the rocky cliffs, a concentrated flow triggers solid-liquid surges routed further downstream along the fan. The debris flows downstream the fan apex are usually subjected to avulsion because of channel plugs caused by stopping small-to moderate-magnitude debris flows. Figure 2 shows the shifting of the active channel after the event of 4 July 2011 (Bernard & Gregoretti, 2021). Other significant events are those that occurred in 2004 and 2006 (Gregoretti & Dalla Fontana, 2008; D'Agostino et al., 2010), both reaching and interrupting the national road SS 51 and those of July and August 2011 (Bernard & Gregoretti, 2021) that reached the cycle path running parallel to the SS 51 at a more elevated location. In July 2013, a major cliff failure interrupted the main debris-flow channel just upstream of the fan apex, and debris flows worked their way through the rocky deposit in the period 2013–2021 (Figure S1 in Supporting Information S1), until on 5 August 2022, a debris flow reached and again interrupted the cycle path following the active channel of 2006 (Figure 1, panel a).

A graphical representation of the most recent historical debris-flow pathways within the considered fan is reported in Figure 2. These pathways were manually digitalized through photointerpretation of aerial images collected between 1952 and 2021, and 8 main active channels have been identified and secondary branches spanning the whole investigated debris-flow fan are identifiable, as reported in Figure 2 panel b, and offered in different colors (from green to red, for the following years: 1954, 1962, 1984, 1991, 1996, 2001, 2006, and 2011, also reported in Figure 1's panel b). In Figure 1, we do not highlight the debris-flow historical pathway related to the flow that occurred in 2021 since it does not significantly differ from the pathways of the one that occurred in 2011.

2.2. Topographic Data and Preliminary Statistics

Our research relies on an Airborne Laser Scanning (ALS)-derived topographic time series, which, from a statistical standpoint, spans a short time window (15 years, from 2006 to 2021), in a discontinuous, incomplete, and heterogeneous manner. Specifically, despite the unavailability of full-detailed survey specifications and official reports, it can be assumed that the employed data were collected in non-consecutive years, on different seasons (i.e., autumn/winter or spring/summer), using different sensors (e.g., full-waveform or discrete returns systems) and acquisition parameters (e.g., flight height or pulse repetition rate). Furthermore, because of the diversity of involved public stakeholders (i.e., Ministry, Region and Local Authorities) as well as private survey companies,

Table 1
Vertical Accuracy of Digital Elevation Model Elevation Data Acquired for Another Catchment in the Fiames Area (BL, Italy)

Survey date	Median (m)	NMAD (m)
2006	0.10	0.43
2010	0.06	0.21
2011	−0.23	0.36
2015	0.02	0.23
2021	−0.02	0.08

the raw data themselves were likely processed differently, that is, by following different pipelines, each employing specific algorithms and software (e.g., Terrascan™ or LAStools™). Nonetheless, despite these limitations relevant from a statistical point of view, the employed topographic time series can be regarded as a typical starting point for any topographic-based, multi-temporal analysis related to debris-flow channels and fans, offering a reliable foundation for evaluating the effectiveness of the proposed methodology. A rough insight into the vertical accuracy of DEMs is reported in Table 1 within the Appendix Section. In contrast, a comprehensive overview of the Airborne Laser Scanner technology, both full-waveform and discrete returns, can be found for example, in Vosselman and Maas (2010), Mallet and Bretar (2009) and Wagner et al. (2006). The available data were collected in different years (and seasons), using different sensors and acquisition parameters. Furthermore, the raw data themselves were processed differently, that is, by following different workflows based on specific algorithms. However, even if not optimal from a statistical perspective, the employed topographic time-frames can be regarded as a typical starting point for any topographic-based, multi-temporal analysis related to debris-flow channels and fans, thus representing a reliable circumstance for testing the effectiveness of the proposed methodology.

Starting from the available ALS data, 5 orthogonal and concurrent multi-temporal DEMs were interpolated for the study area (about 0.8 × 1.1 km) at a grid spacing of 2 × 2 m (about $N = 2 \times 10^5$ pixels details not shown; see Boreggio et al., 2018 and 2022 for further details). Each ith pixel centroid ($i = 1, 2, \ldots, N$) is embedded, for each DEM surface, by its elevation value $z_i = z(\boldsymbol{x}_i)$, located in the centroid coordinates, $\mathbf{x}_i = (x_i, y_i)$. We call it a local elevation difference, $\sigma[z(x_i)] = \sigma(x_i)$, that is, the change at the pixel i in the DEM's elevation. In Figure 3, all the available DEMs are offered as Dem of Differences (DoD), that is, by depicting the elevation differences $\sigma(x_i)$ between each DEM's local elevation (at each pixel $\mathbf{x}_i$, with the spanning index $i = 1$, N) and its 2006 DEM counterpart at the same location. More information about DoDs is given in Figure S2 in Supporting Information S1, where the empirical (i.e., observed) density functions (first row of panels) and cumulated density functions of elevation differences (second row) are included to demonstrate how the DEMs change within the 15 years of measurements, respectively.

Overall, the empirical probability distributions (PDF; second row of Figure S1 in Supporting Information S1, panel b) predictably show an almost normal distribution in 2010 elevation differences, with a median of about 0.0 m. This zero-median value of elevation differences is not unexpected, since it is due to a balance between erosion and deposition volumes, here treated as elevations per pixel units. These differences are almost negligible (<0.1 m) for most of the area, except for locations suffering from high erosion and depositions, that is, those at the feet of the rocky cliff (named fan apex in Figure 1b) and in the proximity of an existing sediment retention basin (see Figure S1 in Supporting Information S1, panel a for details). In fact, by considering that the computational domain represents the entire debris-flow fan, a substantial balance between erosion and deposition volumes is to be expected. On the other hand, the empirical PDFs are more left-skewed for 2011, 2015, and 2021 (median elevation differences of about −0.5 m), thus indicating a substantial erosion tendency (see Figure S1 in Supporting Information S1, panel b). However, a closer look at the elevation differences maps reveals that most of these differences are attributable to inherent noise and alignment problems among the employed DEMs, with spatial patterns having both a low coherence and a low correspondence with the expected ones. Even if this evidence can be regarded as a major drawback for most multi-temporal DEMs-based analyses, as it will be highlighted in Section 2.3, the proposed methodology takes advantage of any morphological variation predicted at the pixel scale by the elevation differences maps, regardless of whether it is real or not, since it represents a source of variation that can effectively be exploited within a stochastic framework for the automatic delineation of most probable debris-flow pathways. As a result, no further pre-processing of the available topographic data was performed before the presented analyses.

2.3. Stochastic Framework for Debris-Flow Pathways

We performed a simulation campaign with three different simulation scenarios, each differing from the others based on the starting DEMs used: *scenario 1* (employed DEMs: 2011 and 2021), *scenario 2* (employed DEMs: 2011, 2015, 2021), and *scenario 3* (employed DEMs: 2006, 2010, 2011, 2015, 2021). Such a grouping of

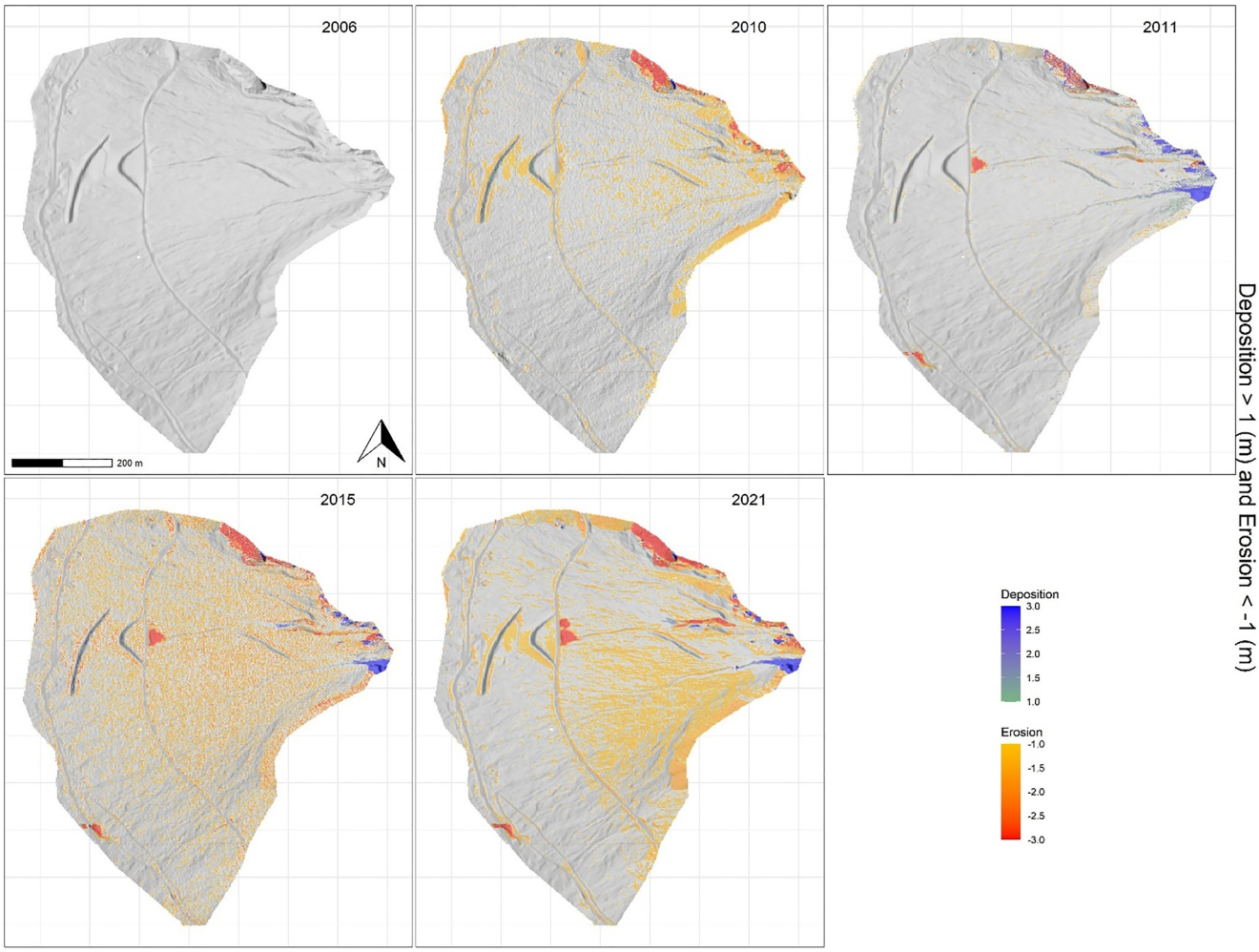

Figure 3. Historical Digital Elevation Model information from 2006 to 2021, depicted by differences from 2006 in meters, as Dem of Differences. Here we depict only significant erosion and deposition elevation changes, that is, those exceeding a local elevation of 1 m, respectively. This eases the identification of the areas more prone to erosion or deposition across the 5 DoDs. The elevation difference cutoff values have been chosen to highlight major erosion and deposition volumes.

topographic data has been done to ensure the widest possible variability in local elevation values, that is, at the pixel scale. In this way, we want to analyze also the impact of a different volume of input information, that is, DEMs, on the generation of stochastic terrains. Therefore, in Scenario 1 we started by employing the most different DEMs upon their elevation CDF, that is, those monitored in 2011 and 2021, and progressively involving the other available DEMs (2006, 2010, and 2015) in Scenario 2 and 3. For each simulation scenario, if m are the starting DEMs involved in calculations (e.g., $m = 2$ and 6 in Scenario 1 and 3, respectively), the local elevation an, $\mu(x_i)$, and standard deviation, $\sigma(x_i)$, are calculated among the m elevation values corresponding to the pixel i. Then, for each scenario, we postulate that possible (synthetic) elevation values are Gaussian-distributed, hence their empirical distribution is fully acknowledged once $\mu(x_i)$ and $\sigma(x_i)$ are known at each pixel i. This assumption of a Gaussian distribution for building probability density functions based on field data is widely employed in geostatistical and geoscience applications (see e.g. Guadagnini et al., 2020 for a different variable; Schiavo, 2022, 2023 for permeability values; Schiavo et al., 2022 for elevation values).

Postulating a Gaussian distribution of synthetic elevation is a mathematically-based hyphotesis. Here we can support this hypothesis upon (at least) three argumentations: (a) most processes reach, after a sufficient time for process development, a Gaussian (or Normal) distribution of possible values of a variable of interest (see Rodriguez-Iturbe & Rinaldo, 2001), which is assured by the Central Limit Theorem (see e.g. Stahl, 2006) and is valid across a wide variety of applied mathematics problems. Moreover, (b) several processes related to flow and transport in surface or groundwater bodies (see e.g. Guadagnini et al., 2020; Zehe et al., 2021) fulfill this point of

the discussion. From a more practical viewpoint, (c) the 5 values of local elevations we gathered, at each domain pixel are mostly distributed as a discrete Gaussian distribution, with one of the 5 values close to the average of local elevations (see elevation differences histograms, hence probability density functions, in Figure S1 in Supporting Information S1, panel b: skewness values are low, and elevation differences are almost gaussian). These three considerations let us be confident of assuming this hypothesis even in this context, which falls within the same field of hydrological sciences.

We simulate an ensemble of Monte Carlo simulations of the local elevation of the domain's cells. The generation of random elevation values is performed with a confidence interval ranging from the local mean elevation value, $E[z(x_i)]$, between a total amplitude of $\pm 2\sigma(z(x_i))$. This way, elevation values are synthetically simulated within a 0.95 confidence interval around the local mean $\mu(x_i)$, and are differently evaluated at each pixel. Therefore, this approach simulates a local elevation value $\widetilde{z}_r(x_i)$ at each pixel that does not necessarily coincide with recorded DEM elevations. For each scenario, we simulate a large enough collection of NMC = 1000 MC (see again Ballio & Guadagnini, 2004; Schiavo, 2024 for references) random Monte Carlo realizations of the local DEM's topography.

We considered each MC-realization as (a) a random field, with locally varying elevation patterns. We thresholded each topography simulation (b) upon a prescribed area-based threshold (in pixel units), hence informing about the being exceeded or not and returned a binary statement (1 or 0, respectively). We also considered (c) the ensemble-averaged topographic surface to retrieve, for each simulation scenario, the most probable configuration of the domain; this is possible since within a Gaussian distributed MC-series of realizations, the local average elevation value coincides with the most probable one. This step gives us the chance to move the analysis within the probability domain. This can be explained by introducing an indicator variable as follows:

$$I_r(\mathbf{x}_i) = \begin{cases} 1 & if \;\; A_r(\mathbf{x}_i) \geq thr \\ 0 & if \;\; A_r(\mathbf{x}_i) < thr \end{cases} \quad with\; r = 1, R \tag{1}$$

with $r = 1, R$ being each M realization, $A_r(x_i)$ the local elevation value (considered as a random variable, as in (a) before) simulated for the rth realization at the ith cell of the domain ($i = 1, 2, \ldots, N$), and $I_r(x_i)$ is the value of $I(x_i)$ in rth realization of the ensemble. Thresholding the simulated random variable returns, therefore, a logical (b) statement, as shown in (Equation 1). Then, $\Pr(\mathbf{x}_i)$ was computed as:

$$\Pr(\mathbf{x}_i) = \frac{1}{R}\sum_{r=1}^{R} I_r(\mathbf{x}_i) = \frac{q}{R} \tag{2}$$

with q (an integer between 1 and R) being the number of MC realizations (up a maximum of R) where the indicator variable is equal to one at the ith location, hence exceeding a prescribed area-based threshold. Since the reference density function is Gaussian, the mean, the median, and the mode coincide with the most probable value, that is, with the result of the (Equation 2), as stated in (c). The volume of MC simulations must be enough to ensure the numerical stability of results, which is stated by appraising the stationarity of the first statistical moments of the variable $\widetilde{z}_r(x_i)$ across CM simulations (see e.g. Ballio & Guadagnini, 2004; Schiavo, 2024). Therefore, the indicator $I(\mathbf{x}_i)$ is a random variable that follows a Bernoulli distribution with probability given by $\Pr[I(\mathbf{x}_i) = 1] = \Pr(\mathbf{x}_i)$.

In the end, to derive a digital drainage network, we employ a "*Deterministic 8*" (i.e., D8) routing algorithm for each MC-topographic surface, as often used in the modeling of flows routing along steep slopes (see e.g. Gregoretti et al., 2016; Orlandini & Moretti, 2009; Simoni et al., 2020). In detail, each MC-surface passes through a pit-filling phase, the local extraction of slopes and D8 flow directions, and the quantification of the corresponding drainage area variable, A_i. An overall view of these methodological steps is presented in the flowchart of Figure S3 in Supporting Information S1.

Our stochastic methodology is exploited to simulate in a simplified way the whole spectrum of morphological variations that can occur within a debris-flow fan because of several geomorphic processes (e.g., debris-flow-related erosion and deposition, slope failure and debris plug). The D8 flow routing algorithm is used to define the debris-flow pathways on such randomly perturbed synthetic digital surfaces.

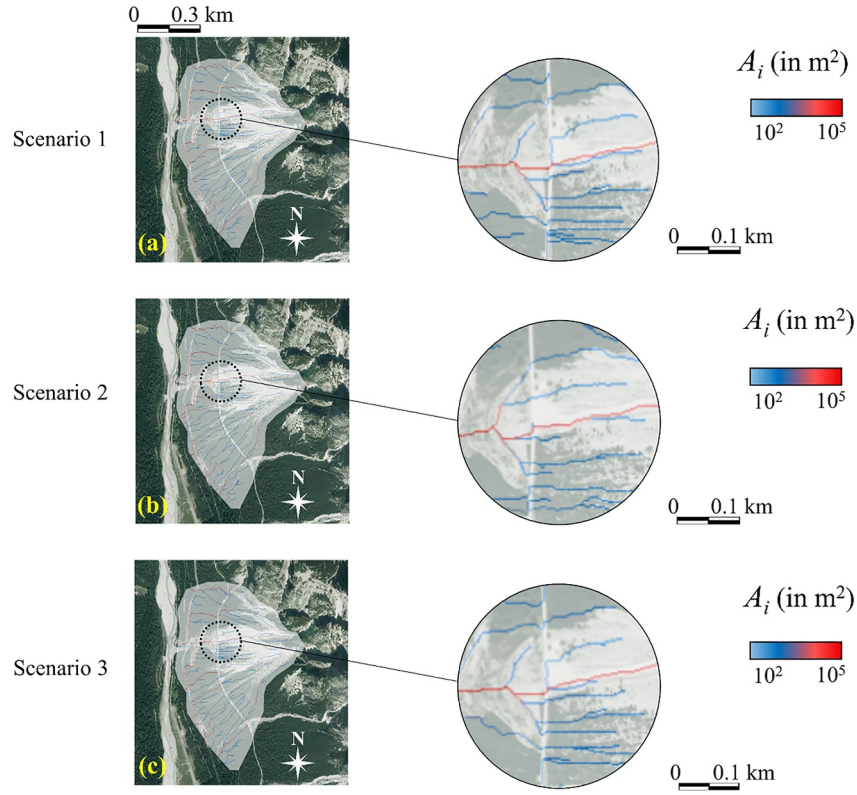

Figure 4. Illustration of one Monte Carlo drainage area simulation for the three employed Simulation Scenarios (panels a–c). As offered in each panel's enlargement, the variation in drainage patterns is relevant only at a large-scale of investigation.

3. Results

3.1. Synthetic Debris-Flow Pathways

The use of synthetic DEMs from the Monte Carlo-based methodology we propose led us to extract as many different networks as possible that debris-flows may route if avulsions occur. Figure 4 illustrates three Monte Carlo drainage area realizations, in squared meters, as examples of outcomes for as many MC-topographies (by columns), for each of the three Simulation Scenarios (by rows), described in Section 2.3. A first appraisal allows us to detect that different simulations within the same scenario do not differ too much from each other regarding the network's topology, as local elevation variations induce only local perturbations in the synthetic simulated terrain, and hence local variations in pathways.

For each simulation scenario tested, the ensemble-averaged topographic surface enables the extraction of the best-estimated drainage area function and returns its most probable result in terms of flow pathways. This is because we employed a Gaussian Distribution (see Section 2.2) to reproduce the multiplicity of possible local elevations throughout the debris-flow fan; hence, the mean value of such a distribution coincides with the median and the mode, and thus with the most probable one. Figure 5 presents the ensemble-averaged drainage area functions for each simulation scenario (by column). Enlargements at the bottom of each panel highlight the scale of variation of this spatial variable among the different tested simulation scenarios. Overall, preferential flow directions remain consistent at the catchment scale, since the variations within the drainage network structure are localized and have no significant impact on full-scale flow directions.

The main strength of the proposed stochastic framework is its ability to shift the identification of debris-flow routes and corresponding spatiotemporal variations (i.e., avulsions) into the probability domain. Figure 6 serves this aim, by illustrating the local probability $\Pr(\mathbf{x}_i)$ of having a possible flow line (hence a pathway) for the transit of a debris flow, hence a routing occurrence, which consists of an avulsion if out of the carved main channel. This probability is extracted starting from a certain drainage area-based threshold (which is subjective;

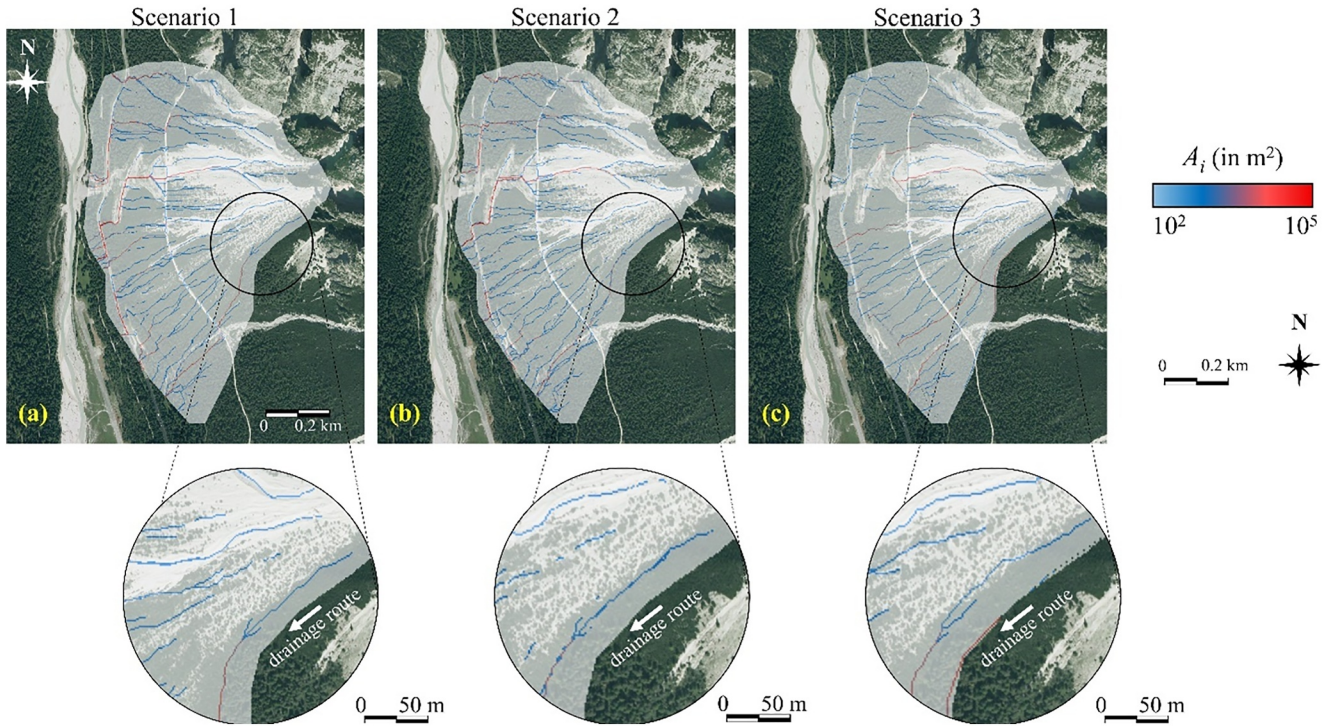

Figure 5. Ensemble-averaged drainage area functions (panels a–c) for each of the three Simulation Scenarios, with enlargements to facilitate the identification of the local probable debris-flow pathway variations.

here we set them at thr = 10^2, thr = 10^3, and thr = 5×10^3 pixels as exemplary ones) imposed on synthetic routing networks of each Simulation Scenario (by column). The lower the threshold, the higher is the likelihood of having a pathway at a randomly selected point of the domain. Conversely, the higher the threshold, the less dense the drainage network becomes; hence, only the major drainage lines are extracted.

3.1.1. Drainage Pathways and Differences Across Different Simulation Scenarios

In Figure S4 in Supporting Information S1 we investigate, for illustrative purposes, one of the most recent events (2011 one, Section 2.1 and Figure 1) by tracing its pathway and plotting the cumulative distribution of the drainage area function (panel b), and that of the occurrence probability of having local conveyances higher than ($A_i > 400$ m^2). Results from different scenarios 1, 2 and 3, are depicted in black, blue, and red lines, respectively. It can be observed that Scenarios 1 and 2 are similar in mimicking the considered historical pathway, as evidenced by their nearly coincident CDFs in both panels a and b for the upstream characteristics of the pathway. This suggests that the two ensemble-averaged DEMs are comparable to each other and return similar drainage patterns. Scenario 3 yields different results, probably due to the employment of DEM information from 2006 to 2011. In any case, the ability of ensemble-average DEMs to replicate the historical pathway is notable, as all three cases return a cumulated probability of about 0.6 at a progressive distance of about 250 m from the pathway's origin (see panel c). This indicates that roughly two-thirds of the pixels belonging to our reconstructed pathways reside on a historical pathway as well.

3.2. Historical and Synthetic Debris-Flow Pathways and Identification of Possible Avulsions

Figure 7 (panels a–c) illustrates historical pathways within the study area, as they have been presented in Figure 2, depicted here in red. These are overlapped with synthetically extracted pathways (the best-estimated ones achieved from the ensemble-average topographic surfaces), based upon a drainage area-based threshold of 4×10^3 m^2, depicted in blue for each Simulation Scenario. First, it can be visually appraised that all the historical pathways resemble some of our synthetic ones. Overall, this can be expected since, in the present research, we are using a set of multi-temporal DEMs covering a later time window than most of the considered historical debris-flow pathways. Therefore, the trace of most of these preferential flow routes is already defined in the employed

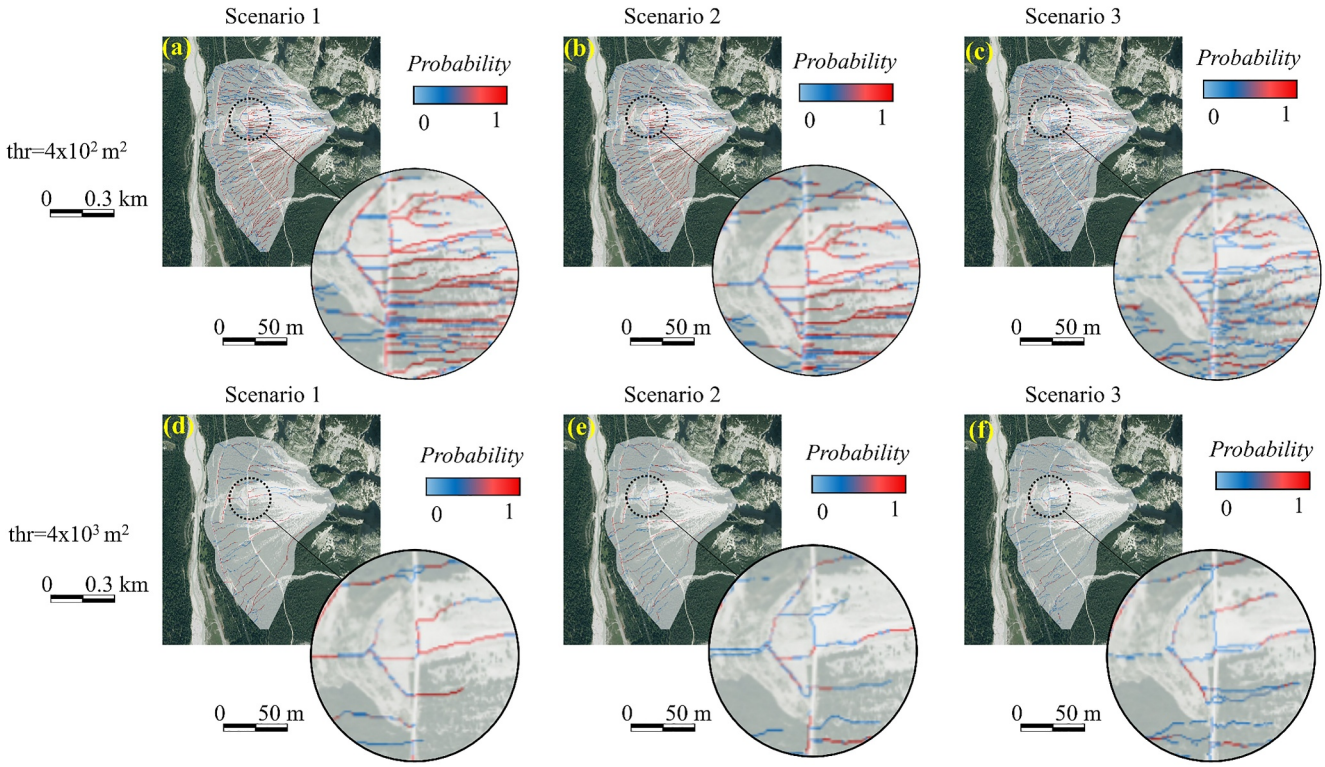

Figure 6. Avulsion probabilistic outcome of stochastic simulations, framed upon different drainage area-based thresholds for each Simulation Scenario (by column). Each probability map is jointly offered with an enlargement of a portion of the computational domain, to ease the identification of local changes in the likelihood of having debris-flow pathways.

digital topographic surfaces. Moreover, as highlighted by Figure 7, apart from spanning the whole considered debris-flow fan, the higher density of synthetic pathways is conveyed in proximity to the historical ones. This can be explained by the fact that local elevation variations have a local impact on each topographic surface. This localized effect is consistent (as highlighted by De Haas, Densmore, et al., 2018) with the fact that avulsions tend to follow pathways that previously occurred in the past since the most probable pathways overlap historical ones and occasionally result in local branching from historical pathways. These results enable us to assess all the possible avulsions that may stem from possible local topographic variations. The best possible match is in the most upstream branch portions, that is, in the initiation part of the flows. Here, the local overlapping between historical (red) and simulated (blue) pathways is very accurate. However, the branching multiplicity is less accurate downstream, since each variation in the DEM may provoke a completely alternative pathway. We use at this stage the overlapping as a metric of goodness, as done by Schiavo et al. (2022), and leave the presentation of further details about the matching likelihood between historical and synthetic (probable) pathways in Section 3.3.

In Figure 7 (panel d), an enlargement of the debris-flow fan apex is offered to ease a large-scale inspection of the location of historical and possible (synthetic) debris-flow pathways. The latter are possible pathways in the case of avulsions occurring in the high-sloping reach of active debris-slow channels, retrieved by our simulations and thus referring to events that have not yet occurred. This is true for all synthetic pathways that do not match with the historical ones, regardless of the considered active channel reach that is, high-, intermediate-, and low-sloping reach; Section 1, whereas in Figure 7 only an example referring to the upstream part of the catchment has been given.

We can prove the consistency of our approach by assessing the good the match is between the most probable synthetic pathways and historical ones. To this aim, Figure S5 in Supporting Information S1 shows a perspective view of the same enlargement offered in Figure 7d. Historical pathways are depicted in red (see e.g., those in proximity to the letter a), and visually match the extracted debris-flow network (overlapped in blue, as in Figure 7's panels). Moreover, the location of possible debris-flow pathways, which are not the historical ones, in

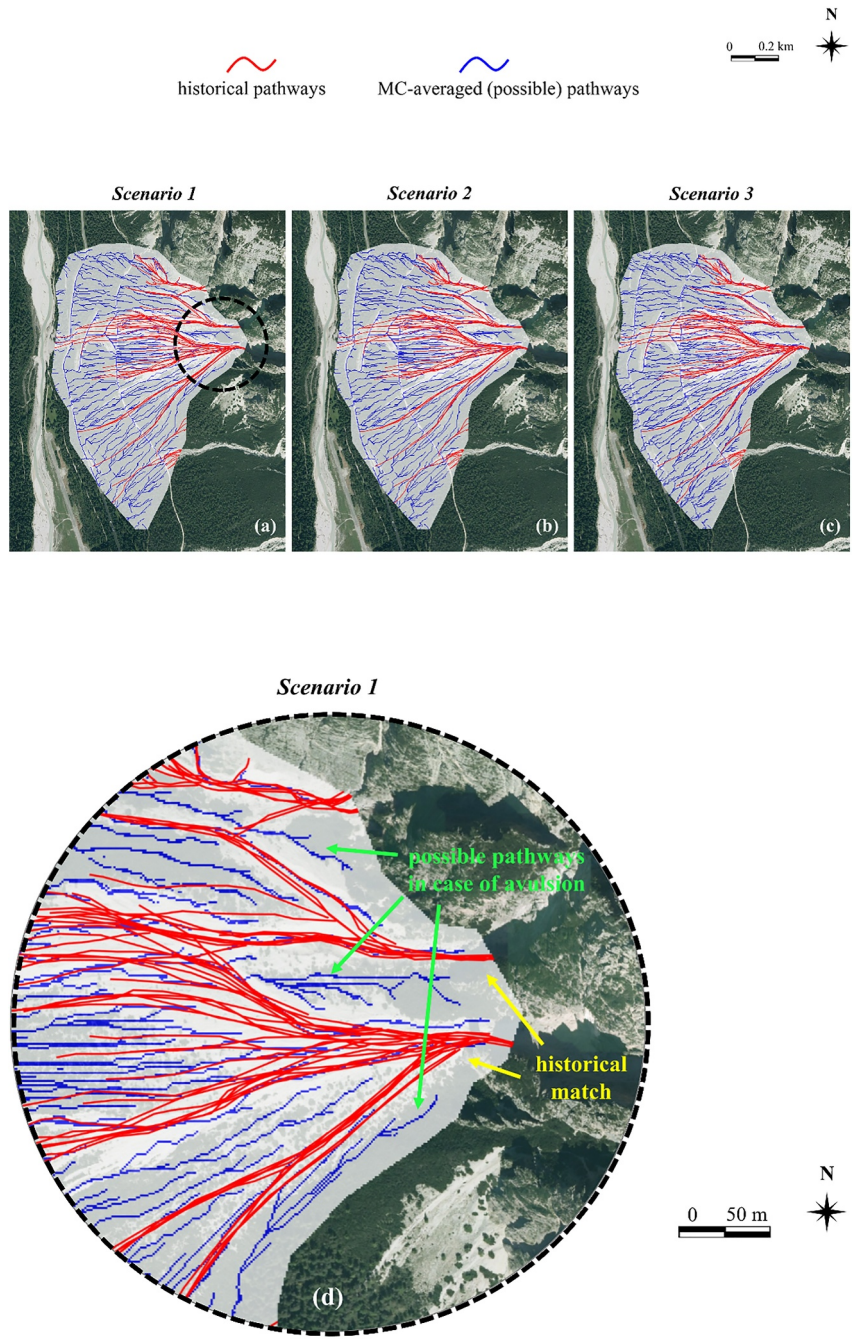

Figure 7. Ensemble-averaged debris-flow pathways (in blue) and historical ones (in red) for each Simulation Scenario (panels a–c), at the debris-flow fan scale. For exemplary purposes, the debris-flow fan apex is enlarged (panel d) for simulation stemming from Scenario 1. The match between synthetic pathways and historically occurred ones, and other possible pathways in the case of avulsions occurring in the high-slope reach of the active channels, are observable.

the case of avulsions is highlighted by letters (b) and (c), for exemplary purposes. Other possible channels can occur where there are morphological shapes that carve the terrain and tend to convey subsequent flow events, such as paleochannels not active within the observation period. In the case of paleochannels, as the one highlighted by (c), they are carved on the employed DEMs, and are in vegetated areas where the local terrain tangential curvature is suitable for possible flow concentration and routing. Of course, the most expectable debris-flow dynamic along

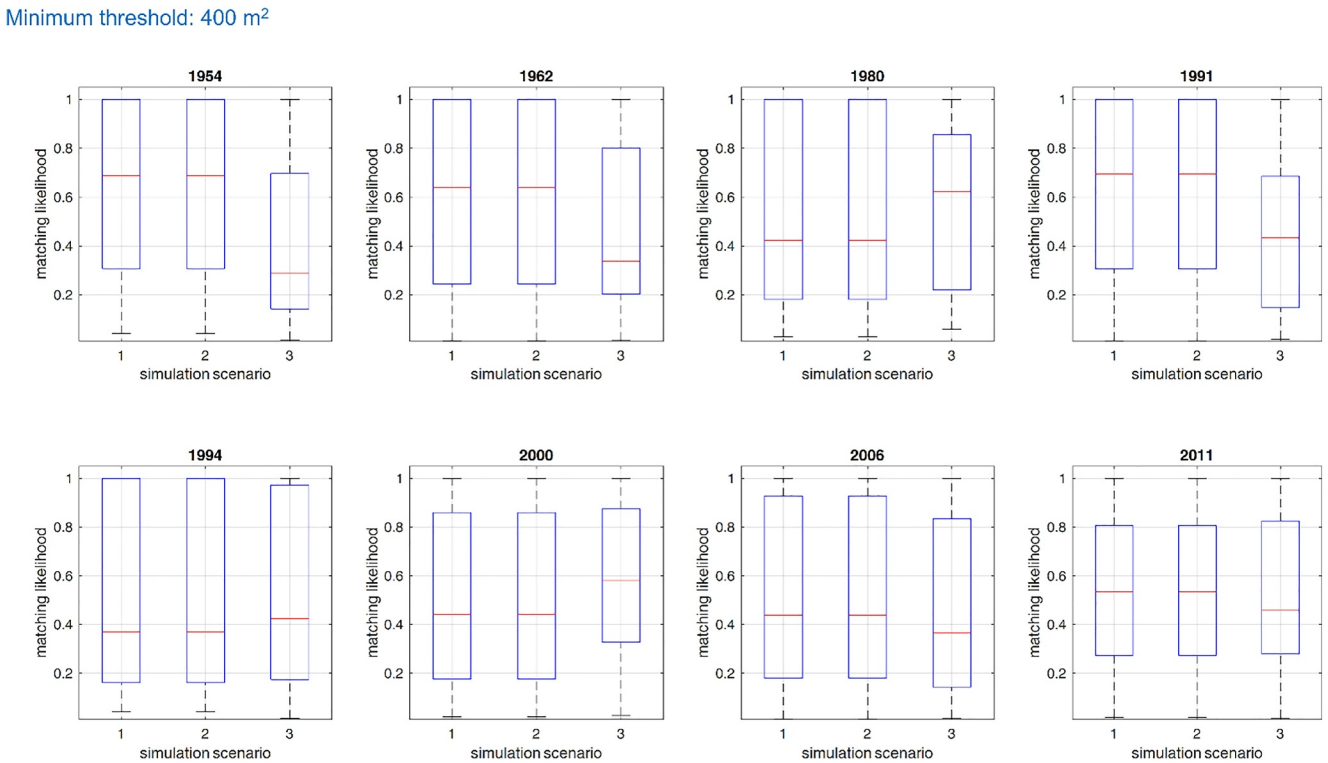

Figure 8. Matching likelihood between historical (i.e., observed) debris-flow pathways and probabilistic (i.e., simulated) ones is estimated by offering the range of variability of local probabilities of occurrence of synthetic pathways (in boxplots, for each Simulation Scenario) along historical routes (one subplot for each route).

these probable pathways, as well as their possible deviation, cannot be fully evaluated by our methodology but must be demanded for further analyses through debris-flow routing models.

3.3. Consistency of Possible Avulsions Along Specific Flow Lines: The Case of Historical Pathways

We now aim at assessing and quantifying the goodness of our approach in reproducing pathways of historically occurred flows (1954, 1962, 1980, 1991, 1994, 2000, 2006, 2011; Figure 2 panel b). As introduced in Section 2.1. These debris-flow main pathways were manually digitalized through photo interpretation of aerial images collected between 1952 and 2021 by the Mountain Hydrology group at the University of Padova in the previous years (see Acknowledgments). It is therefore worth keeping in mind that these linear features represent only the rough trace of the most recent main flow directions and not the thalweg of the active channels themselves. Although these identified features may be prone to local hand-made digitalization errors, they serve here to our purpose of quantifying if high discrepancies arise between our probabilistic delineation of debris-flow pathways and historical ones.

We compare the spatial location of each of the 8 yearly historical pathways with our probabilistic outcomes, the latter ones obtained from each Simulation Scenario and previously thresholded upon a minimum drainage area of 400 m^2 (arbitrarily chosen for exemplary purposes, and consistent with Section 3 results). Then, we quantify the likelihood of matching a yearly historical pathway by calculating the probability of having a synthetic pathway in pixels where historical ones occurred. We estimate this likelihood by assessing the local probability of occurrence of synthetic pathways (properly thresholded) along historical pathways, where the local (historical) occurrence probability within the period 1954–2011 is equal to 1. This way, the higher the local probability, the closer our spatial (probabilistic) reconstruction of possible pathways, hence the higher the consistency of our probability outcomes of locally resembling observed historical pathways. The following Figure 8 illustrates, for each yearly pathway, the likelihood of matching our simulations. As can be appraised by boxplots, the matching likelihood varies upon the year (a subplot for each one) and the Simulation Scenarios (on plots' *x*-axis) which are employed in the spatial comparison.

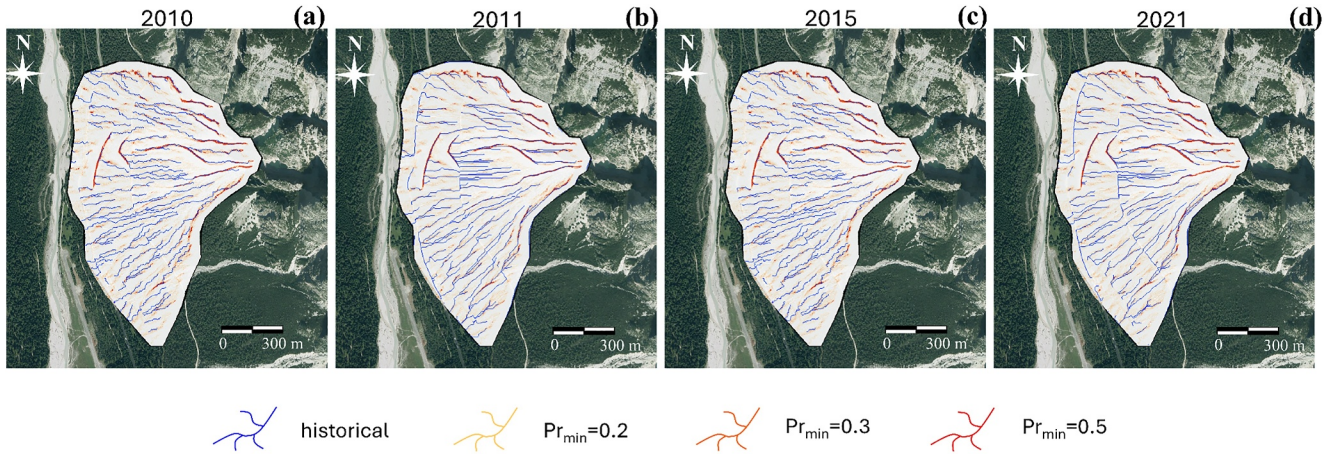

Figure 9. Predicting digital pathways (from the 2010, 2011, 2015, and 2021 Digital Elevation Models) by perturbating the 2006 one. Predicted pathways are offered in colors upon a minimum occurrence probability across the MC ensemble of simulated ones, while the observed digital ones overlap in blue.

3.4. Predicting Future Debris-Flow Avulsions

Our stochastic framework can also be employed in a predictive perspective. To do this, we take the first available DEM (the 2006 one) and we stochastically perturb its topography to achieve multiple possible perturbed terrains by imposing on each DEM's pixel a random vertical perturbation (between −4 and +4 m), with a sensitivity of 0.05 m. This local elevation change range was taken from the 95% confidence interval of CDF's variations retrieved from all 5 DEMs of the available time series (Figure 2, Section 2.2, and overall it can be regarded as a reliable representation of the morphological variations that can occur within a debris-flow fan as a consequence of different geomorphic processes (e.g., debris-flow-related erosion and deposition, debris plug formation, and rockfall- or snow avalanches-related deposit). For each synthetic DEM, we then repeat the procedure of extracting the routing pathway, through the D8 flow algorithm. In this way, we want to see if perturbating the initial DEM is possible to reproduce the debris-flow pathways and corresponding variations (i.e., avulsions) that occurred later in the investigated time window of debris-flow fan evolution. A positive outcome from this analysis would sustain the predictive ability of our framework, and its possible applicability also with only 1 DEM. Perturbating the 2006 DEM led us to collect an ensemble of synthetic DEMs and hence, an ensemble of possible pathways. The latter can be collected and treated in a probabilistic way. An ensemble of 2000 MC realizations of 2006-perturbated terrains is simulated. The higher volume of MC simulations concerning the previous ones is due to the less input information, which requires more simulations to ensure the numerical stability of results (see the Section 2).

The following Figure 9 illustrates the spatial match with the digital pathways that can be retrieved by the DEMs available for 2011, 2015, and 2021 flows, and extracted upon an area-based threshold of 800 m^2, that is, pixels (panels a–d). These are superimposed to probable synthetic pathways, extracted with the same threshold, offered upon three minimum occurrence probability thresholds: 0.2 (in yellow), 0.3 (in orange), and 0.5 (in red). The overall appraisal of the spatial patterns of our predictive synthetic simulation allows us to assess the ability to match a good number of historically occurred pathways. Figure S6 in Supporting Information S1 (panels a and b) depicts the matching likelihood between historical and predicted pathways for each available DEM and upon the three probability thresholds. As it can be appraised, more probable pathways have higher chances of being predicted by perturbating an antecedent DEM. The matching likelihood is stable when predicting pathways across the whole investigated temporal window, due to the poor variability from 2011 to 2021.

3.5. Predicting Future Pathways: The Case of the 2011 Avulsion

We detail this worthy kind of results by offering to the reader the following Figure 10. In panel, a, the pathways obtained from perturbating the 2006 DEM are highlighted in orange and red color if exceeding a minimum occurrence probability of 0.3 and 0.5, respectively. We overlap with these the spatial reconstruction of the historical avulsions that occurred in 2011, whose tracks are highlighted in light blue, while the previous channel (before any avulsion) had a track that has been highlighted in green. We can see 3 main avulsions, been carved

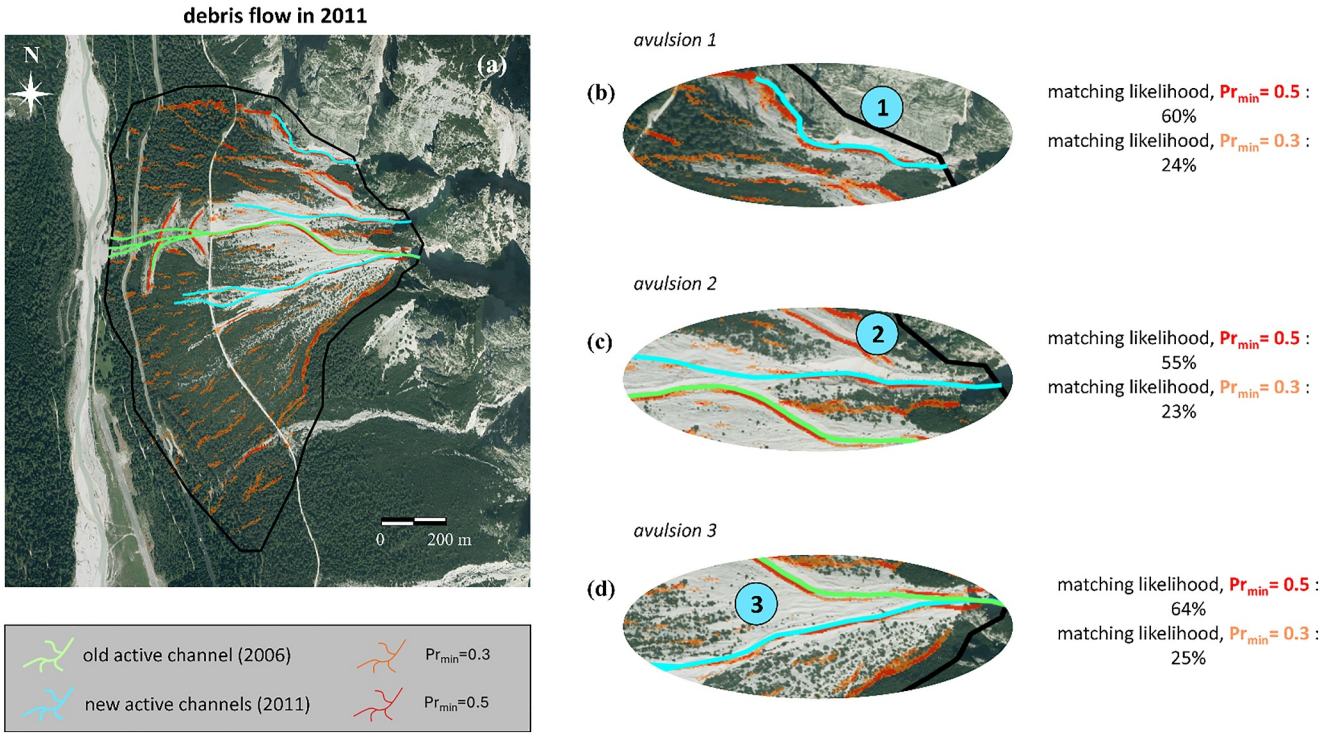

Figure 10. Spatial prediction of the avulsions (a) occurred after the 2011 flow, obtained by perturbating the 2006 Digital Elevation Model. While the previous channel is offered in green, new avulsion pathways are offered in light blue. Insets b-d enable a detailed appraisal and quantification of the matching likelihood between historical avulsion and synthetic pathways, thresholded upon a minimum occurrence probability of 0.3 (in orange) and 0.5 (in red).

within the fan as flow's preferential channels of propagation downslope. In the enlargements (panels b–d), we analyze each of these pathways and estimate the matching likelihood with the pathways obtained from the ensemble we mentioned before. We calculated the likelihood of predicting the same pathway of these avulsions upon using the 2006 DEM of 55%–64% and 23%–25% considering synthetic pathways with minimum probabilities of 0.5 and 0.3, respectively. It is worth underlying that the upstream part of the avulsions' tracks resembled better than the downstream parts, and this is reasonable because the more downslope within the catchment, the higher the spatial meandering of the avulsion channel, and this increases the difficulty of its exact spatial prediction. In the end, we remark that we obtained similar results for all the historical avulsion pathways shown in Figure 2, although we only offer the last one for exemplary purposes.

4. Discussion

In our research, we rely on topographic data and employ them from a statistical perspective for gridding a set of concurrent DEMs of an alpine debris-flow fan, from which a consistent volume of synthetic digital surfaces and related drainage patterns are extracted. The aim is to test the effectiveness of a simplified and topographic-based digital strategy for the automatic delineation of probable debris-flow pathways and hence possible avulsions, within a stochastic perspective. In detail, starting from the available DEMs, three different simulation scenarios were defined by using an increasing number of topographic information, and several Sequential Gaussian Simulations were performed based on the morphological variation observed within the study area in a limited time window of 15 years.

The inherent characteristics of available time series do not allow the statistical testing of the suitability of the employed analytical model; it is worth noting that this assumption is widely used in stochastic simulations of geomaterials (Deutsch & Journel, 1998), contamination pathways (Zehe et al., 2021), diffuse contamination (Schiavo, Giambastiani, et al., 2024), or natural background levels (see e.g. Guadagnini et al., 2020), or elevation measurements (Schiavo et al., 2022). The probabilistic outcomes presented in Section 3.1 highlight that the extracted synthetic networks are in good agreement with the most recent historical debris-flow pathways observed

within the investigated spatial domain (Figures 6 and 7). Moreover, the stochastically generated probable debris-flow routes show weak spatial variations at a small scale of inspection, with only local changes in the possible flow directions, as shown in Figures 4 and 5, and in Figure 5S. This means that the stochastically defined locations that are more likely to reside on a debris-flow routing path are similar to existing channels. This lets us understand that even in case of significant elevation changes within the considered spatial domain (i.e., within a 95% confidence interval), the flows will likely follow some preferential pathways, which are mostly located along the observed historical channels. Conversely, other areas of the considered debris-flow fan are susceptible to channel avulsions with lower occurrence probabilities (i.e., only a limited number of simulations show flow occurrence). Thus, only major erosion and deposition phenomena can alter the existing terrain morphology in a way to produce a significantly different pathway, in general agreement with the observed physical phenomenon (i.e., debris plug formation and subsequent shifting of the shifting of an active channel throughout the fan surface). This behavior can also be explained from an energetic viewpoint, since the most favorable condition for debris flows is to maximize the local potential energy drop (see e.g. Howard, 1990; Orlandini & Moretti, 2009; Schiavo et al., 2022) follows an existing steepest descent pathway, according to the gravity-driven routing we employed (i.e., the D8 algorithm). Local elevation (i.e., energetic) variations may not have the magnitude to perturbate the active pathway as much as the energy required to provoke a significant avulsion, and thus an active channel shifting. Anyway, despite its simplicity, our framework is proved to be able to identify both the most probable pathways and the possible avulsions (see Figures 7 and 8, and Figure S4 in Supporting Information S1).

In Sections 3.1 and 3.1.1, we strengthen the concept that pathways mostly recur in the same areas and avulsions occur with lower chances by inspecting probabilities of having a synthetic pathway along a historical route (the 2011 one). As shown in Figure S4 in Supporting Information S1, the cumulative probability of occurrence of synthetic pathways is not so different among the tested simulation Scenarios, since the three CDFs mostly behave similarly along the considered flow route. This means that the field of occurrence probabilities along that pathway is quite stable to possible variations due to the use of different topographic input data to simulate MC terrains. The 2011 pathway has been taken as an exemplary case study, and similar results can be obtained for other ones as well.

In Section 3.3 we further analyzed the spatial overlapping between the historical pathways (8 main flow routes detected from 1954 to 2021, and manually digitalized by our group in previous years) and our probabilistic outcomes, for each of the three tested Simulation Scenarios. In detail, we compare the (certain) occurrence of flows along historical pathways, where we are sure that flows occurred in the past, with the probability of having synthetic pathways on the same routes. In Figure 8, we aimed to assess how pathways referring to the 1954 and 1962 flows retain the highest difference with the simulated networks, that is, with the occurrence probability we can retrieve from our probable ones. This is clear when inspecting probabilities obtained by using the latest surveys in simulating terrain (i.e., the 2015 and 2021 ones), and thus extracting flow pathways. The resulting pathways are quite unlikely to match the oldest ones (e.g., the 1954 one, with an average $Pr = 0.3$). Conversely, more recent flows (e.g., the 1991 or 2006 one) reside on pathways that are more likely to match those that can be inferred by employing the latest DEMs, with the matching likelihood that they can reach $Pr = 0.7$ and $Pr = 0.6$ for Scenarios 1 or 2 and 3, respectively. This result is highly informative about the spatial discrepancy in pathways between historical and recent flows, as well as being informative about the use that one can make of available information and surveys.

In Section 3.4, we tried to understand if our framework can also be employed in a predictive manner. In detail, we randomly perturbed the first DEM (2006) of the available topographic time series (i.e. 2006 one, with elevation perturbations of ± 4.0 m) with an MC procedure and see if it is possible to match the pathways that can be digitally extracted by subsequent DEMs (i.e., 2010, 2011, 2015, and 2021). The results in Figure 9 are encouraging: high probability occurrence thresholds (e.g., $thr = 0.5$) enable us to identify only the most probable avulsion pathways. In the best cases, 55%–64% of these overlap the flow lines extracted from the 2010 to 2021 DEMs. Conversely, lower occurrence probability thresholds (e.g., 0.2) return lower matching likelihoods (about 7%). Thus, the drainage area-based and the probabilistic thresholds employed in extracting networks play a critical role in this sense and in the prediction of pathways upon antecedent DEMs.

In Section 3.5, we offer a supplementary insight related to the predictive ability of our methodology by inspecting (see Figure 10) how good the match between historical avulsions that occurred since 2011 flow and those retrieved from the most probable pathways obtained before. The results are encouraging since up to 64% of pixels belong to a pathway with a minimum occurrence probability of 0.5 overlap flow lines belonging to the 2011 route.

All kinds of results offered in Sections 3.3, 3.4, and 3.5 should be carefully considered. Although we underline how the probability of predicting possible future avulsions depends (a) on the number of DEM employed, (b) on the quality of data that enabled these survey-based products, (c) and on the drainage area and (d) probability thresholds employed for delineating pathways within the MC framework (the latter two are arbitrary). Nevertheless, these results are important concerning the task of future avulsion prediction. As said before, the main flow pathways remain stable in space (i.e., throughout the study area) across the whole-time window, so the low matching likelihood is mostly due to the inaccuracy in capturing secondary avulsion branches, with the main channels well predicted also by employing only the 2006 terrain survey.

Furthermore, here we acknowledge how this result stems from the energetic nature of the debris-flow phenomenon, which, even in an unconfined environment featured by high-slope conditions, implies quasi-uni-unidimensional flows that rarely diverge from the main flow directions. This finding represents an important research outcome since, despite its inherent simplicity in reproducing the complex phenomenon of flow avulsion in an unconfined environment, our methodology can be a suitable tool for digital elevation data users involved in debris-flow risk modeling and mitigation tasks. In this sense, our results are consistent with what we discussed, since the most probable pathways follow historical routes, and sometimes (i.e., for a limited number of MC realizations) they diverge from usual pathways, and avulsions from the main channels occur.

After discussing Sections 3.3, 3.4, and 3.5, we want to highlight that this kind of result should be adapted, for other case studies or catchments to be investigated, to available data, and the local density of the network. This means that the probability thresholds we employed, as well as the area-based thresholds we employed for extracting the debris-flow networks, can be decided by the user. These parameters are sensitive to the local case study and may depend on the researcher's experience in another study area. For our case study, we chose these parameters relying on available data and our experience in the field and surveying to give an idea of the kind of results one can come up with. Moreover, the choice of proper area-based and probability thresholds also depends on the morphology of the catchment. For example, highly incised catchments, with main channels carved in rocky fans are very less susceptible to historical elevation variations, hence the MC outcomes won't give highly variable terrains, at least in these areas, thus the suitable area and probability threshold values can be high. Our methodology surrogates erosion and deposition phenomena, and in particular their localized effects on the terrain topography, by simulating local random elevation variations, that is, simulating possible erosion (if the variation is negative) or deposits (if the variation is positive) within a feasible confidence data-grounded interval. Moreover, debris fans are highly prone to temporal elevation (hence, morphological) variations that should be treated both in the probabilistic and prediction perspectives with lower thresholds. In all these cases, probable debris flow pathways are located within debris fans, where the fan is covered by shrubs, or where the local concave terrain suggests the presence of paleochannels that can be flooded by future flows.

Several research questions stem from the perspective we described, even in different application fields of hydrological sciences. Nowadays, researchers are trying to quantify and identify the migrations of the drainage divides upon high-resolution topographic data, like those we employed (see e.g. Zhou et al., 2024), and the spatial patterns of dynamic migration of channels in highly-varying terrains (see e.g. Abdollahi et al., 2024; Boulton et al., 2024; Yaaqoub & Essaifi, 2023). Therefore, the application of novel stochastic concepts and approaches within the debris-flow "world," which usually relies on field surveys for pre-event and post-event flow assessment or landscape vulnerability (see e.g. Barnhart et al., 2021), may lead us to propose a novel work to be framed within the most recent research concepts and vectors in the field. Relying on these literature references, in the future, we could consider a landscape evolution model to envelop different DEM information and to predict future terrain surfaces and hence pathways. In the present context, a representative spectrum of possible topographic configurations (Bonetti et al., 2020) can reproduce a wide variety of channel shifting and avulsions (e.g., De Haas, Densmore, et al., 2018), triggered by a sequence of flows or by intense erosion or deposition phenomena. We believe that borrowing this novel perspective allows us to shed light on a catchment vulnerability to debris flows and quantitatively identify the morphological complexities of the terrain (Forte et al., 2016).

Overall, based on the presented results, the volume and the quality of available topographic data are important for the present framework, but not essential. The proposed methodology can also be replicated in the case of a few pieces of information, or even in the extreme condition of having a single DEM available for a study debris-flow prone area, as we shown in Section 3.4 and 3.5. In other words, if only one DEM is available, a stochastic and evidence-based random perturbation of the available topographic surface would be a suitable option for generating

several Monte Carlo synthetic DEMs, and for employing the proposed approach. Of course, this might not be strictly adherent to the physical reality that can be observed in a debris-flow area, where the highest elevation differences due to erosion and deposition processes are usually located at the fan apex (see e.g. Simoni et al., 2020; Tiranti et al., 2018).

5. Conclusions

We set up a framework for delineating debris-flow pathways on fans, where avulsions from the active channel can occur, from a probabilistic perspective. We leveraged several surveys to extrapolate local elevation data for simulating stochastic synthetic Monte Carlo terrains starting from available DEMs. We then employed commonly used routing algorithms for each synthetic terrain simulation to extract channel networks and to treat them from a probabilistic viewpoint. These channel networks are possible flow pathways routed by debris flows after the occurrence of avulsions. The major results of the work can be summarized as follows:

- We analyzed a fan of the Dolomites where avulsions from the active channel frequently occur, and of which, five LiDAR-based DEMs are available (2006, 2010, 2011, 2015, and 2021). We identified all the avulsions and the corresponding debris-flow pathways that occurred in the period 1954–2021 through the observation of orthophotos. The observed debris-flow pathways exhibited significant variations, so all the fan surfaces have been interested in past debris-flow propagation.
- We set up our analysis from three different combinations of the available DEMs, that is, using 2,3 or 5 DEMs as input data to generate a collection of Monte Carlo synthetic terrains. From each one of these terrains, we retrieve a flow network. Using all the flow networks as an ensemble, we can map the probability that a pathway after an avulsion may occur within the catchment.
- We assessed whether our results were feasible by quantifying the matching likelihood between historical and preferential synthetic pathways. This allows us to assess the feasibility of our method for detecting which pathways may be followed by the flow after an avulsion. We found median matching likelihoods between synthetic and historical pathways within a range of 45%–75%, with slight differences among scenarios 1, 2, and 3.
- We employed our framework in a predictive way. We demonstrated that the employment of the 2006 DEM, that is, just 1 of the 5 DEMs we have, enabled us to capture major pathways carved on DEMs between 2011 and 2021 (Figure 9). We found matching likelihoods between 55% and 64% for pathways with a minimum occurrence probability of 0.5, which enables to identify preferential alternative pathways.
- We employed the same methodology to capture the avulsion pathway of the debris flow that occurred in 2011 (Figure 10). In this case, we found a 64% match when using a probability threshold of 0.5.

In the end, we employed a stochastic approach, borrowing some concepts from other disciplines, for achieving probabilistic maps of debris-flow pathways to capture the routes followed by debris flows after the avulsions from the active channel. Our framework allows the capture of the historical main avulsion pathways that occurred within the study area and can be used for the prediction of future possible avulsions. This is a very important outcome so that the proposed framework can be employed in the risk-assessment study of fans routed by debris flows and in the planning of control works. Further research vectors should explore other approaches, for example, via spatiotemporal variogram-based modeling of elevation perturbations to be assigned to one or more available DEMs, when creating the synthetic ensemble of terrains.

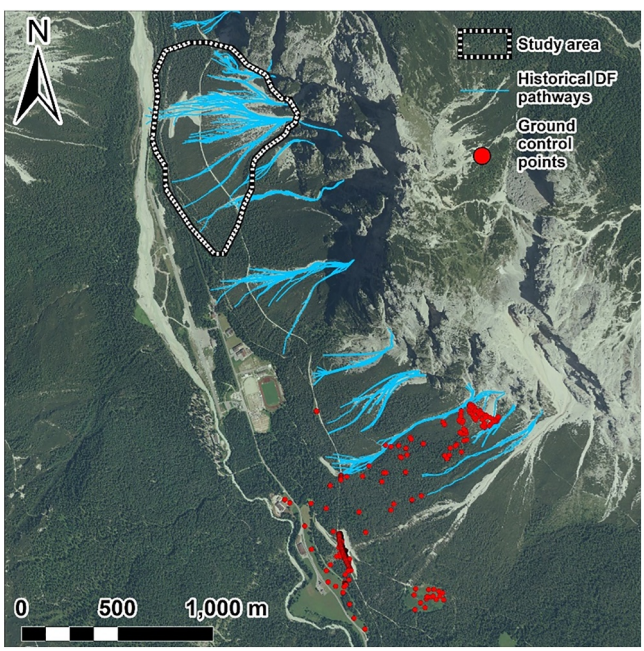

Figure A1. The area where Ground Control Points were taken in 2015 (red dots) and all debris pathways in the Cortina d'Ampezzo area (in light blue).

Appendix A: Airborne Laser Scanning

The vertical accuracy data reported in Table 1 were computed by comparing the DEM elevation data against 566 RTK-based GNSS point measurements acquired on well-distributed stable areas (e.g., big boulders, roadways, hydraulic defense works, not debris-flows affected areas, etc.) by the research group in December 2015 in a nearby study area (see Figure A1). Considering

the significant spatial variability of the vertical error in DEMs, metrics such as the median error value (median, in Table 1) and normalized mean absolute difference (NMAD, in Table 1) must be considered as a rough estimate of the actual vertical accuracy of employed DEMs within the study area. Furthermore, no reliable information about horizontal accuracy can be provided, because of the inherent complexity in estimating the horizontal errors of DEMs. Overall, a rough estimate can be computed as a factor of the flight height (typically from 1/800 to 1/1000, depending on the employed sensor). However, even these rough estimates of the horizontal error cannot be provided due to the unavailability of full-detailed survey specifications and official reports (apart from the 2015 survey). Similarly, no detailed information about raw data collection and processing can be provided.

DEM vertical error statistics were computed after Höhle and Höhle (2009). Please note that the vertical accuracy of data was obtained by comparing the DEM elevation data against 566 RTK-based GNSS point measurements acquired on well-distributed stable areas (e.g., big boulders, roadways, hydraulic defense works, not debris-flows affected areas, etc.) by the research group in December 2015 in a nearby study area. We can employ some metrics to consider the spatial variability of the vertical error in DEMs as a rough estimate of the actual vertical accuracy of employed DEMs within the study area. Furthermore, no reliable information about horizontal accuracy can be provided, because of the inherent complexity in estimating the horizontal errors of DEMs and the unavailability of full-detailed survey specifications and official reports.

Data Availability Statement

The data on which this article is based are available in Schiavo, Gregoretti, et al. (2024). Both data and the MATLAB code to perform our simulations are open-access and freely available.

Acknowledgments

This study was carried out within the RETURN Extended Partnership and received funding from the European Union Next-GenerationEU (National Recovery and Resilience Plan – NRRP, Mission 4, Component 2, Investment 1.3 – D.D. 1243 2/8/2022, PE0000005). It also relied on the previous research carried out in the following projects: "GAPDEMM (GIS-based integrated platform for Debris-flow Monitoring, Modeling and Hazard Mitigation," funded by CARIPARO foundation); "PARAmount (imProved Accessibility: Reliability and security of Alpine transport infrastructure related to mountainous hazards in a changing climate)" funded by Alpine Space program of European Union; The authors would like to thank the association "Regole d'Ampezzo" the Department of Land Defense and Civil Protection of the Province of Belluno for providing LiDAR data sets of 2010 and 2011, respectively. Lastly, a special thank to Massimo Degetto for the digitalization of the historical debris-flow active channels. Open access publishing facilitated by Universita degli Studi di Padova, as part of the Wiley - CRUI-CARE agreement.

References

Abdollahi, M., Vahedifard, F., & Leshchinsky, B. A. (2024). Hydromechanical modeling of evolving post-wildfire regional-scale landslide susceptibility. *Engineering Geology*, *335*, 107538. https://doi.org/10.1016/j.enggeo.2024.107538

Anand, S. K., Bertagni, M. B., Drivas, T. D., & Porporato, A. (2023). Self-similarity and vanishing diffusion in fluvial landscapes. *Proceedings of the National Academy of Sciences of the U S A*, *120*(51), e2302401120. https://doi.org/10.1073/pnas.2302401120

Baggio, T., Martini, M., Bettella, F., & D'Agostirno, V. (2024). Debris flow and debris flood hazard assessment in mountain catchments. *Catena*, *245*(108338), 108338. https://doi.org/10.1016/j.catena.2024.108338

Ballio, F., & Guadagnini, A. (2004). Convergence assessment of numerical Monte Carlo simulations in groundwater hydrology. *Water Resources Research*, *40*(4), W04603. https://doi.org/10.1029/2003WR002876

Barbini, M., Bernard, M., Boreggio, M., Schiavo, M., & Gregoretti, C. (2024). An alternative approach for the sediment control of in-channel stony debris-flows with an application to the case study of the Ru Secco Creek (Venetian Dolomites, Northeast Italy). *Frontiers in Earth Science*, *12*. https://doi.org/10.3389/feart.2024.1340561

Barnhart, K. R., Jones, R. P., George, D. L., McArdell, B. W., Rengers, F. K., Staley, D. M., & Kean, J. W. (2021). Multi-model comparison of computed debris-flow runout for the 9 January 2018 Montecito, California post-wildfire event. *JGR: Earth Surface*, *126*(12). https://doi.org/10.1029/2021JF006245

Bernard, M., Barbini, M., Boreggio, M., Biasuzzi, K., & Gregoretti, C. (2024). Deposition areas: An effective solution for the reduction of the sediment volume transported by stony debris-flows on the high-sloping reach of channels incising fans and debris cones. *Earth Surface Processes and Landforms*, *49*(2), 664–683. https://doi.org/10.1002/ESP.5727

Bernard, M., & Gregoretti, C. (2021). The use of rain gauge measurements and radar data for the model-based prediction of runoff-generated debris-flow occurrence in early warning systems. *Water Resources Research*, *657*(3), 1–27. https://doi.org/10.1029/2020WR027893

Berti, M., & Simoni, A. (2005). Experimental evidences and numerical modelling of debris flow initiated by channel runoff. *Landslide*, *2*(3), 171–182. https://doi.org/10.1007/s10346-005-0062-4

Bonetti, S., Hooshyar, M., Camporeale, C., & Porporato, A. (2020). Channelization cascade in landscape evolution. *Proceedings of the National Academy of Sciences of the U S A*, *117*(3), 1375–1382. https://doi.org/10.1073/pnas.1911817117

Boreggio, M., Bernard, M., & Gregoretti, C. (2018). Evaluating the differences of gridding techniques for digital elevation models generation and their influence on the modeling of stony debris flows routing: A case study from Rovina di Cancia Basin (North-Eastern Italian Alps). *Frontiers of Earth Science*, *6*. https://doi.org/10.3389/feart.2018.00089

Boulton, S. J., Rodés, A., Fabel, D., Alçiçek, M. C., & Whittaker, A. W. (2024). Complex erosional response to uplift and rock strength contrasts in transient river systems crossing an active normal fault revealed by 10Be and 26Al cosmogenic nuclide analyses. *Earth Surface Processes and Landforms*, *49*(4), 1428–1450. https://doi.org/10.1002/esp.5778

D'Agostino, V., Cesca, M., & Marchi, L. (2010). Field and laboratory investigations of runout distances of debris flows in the Dolomites (Eastern Italian Alps). *Geomorphology*, *115*(3–4), 294–304. https://doi.org/10.1016/j.geomorph.2009.06.032

De Haas, T., Densmore, A. L., den Hond, T., & Cox, N. J. (2019). Fan-surface evidence for debris-flow avulsion controls and probabilities, Saline Valley, California. *J. Geophys. Res.Earth Surface*, *124*(5), 1118–1138. https://doi.org/10.1002/2018JF004815

De Haas, T., Densmore, A. L., Stoffel, M., Suwa, H., Imaizumi, F., Ballesteros-Canovas, J. A., & Wasklewicz, T. (2018). Avulsion and the spatio-temporal evolution of debris-flow fans. *Earth-Science Reviews*, *177*, 53–75. https://doi.org/10.1016/j.earscirev.2017.11.007

De Haas, T., Kruijt, A., & Densmore, A. (2018). Effects of debris-flow magnitude frequency distribution on avulsions and fan development. *Earth Surface Processes and Landforms*, *43*(13), 2779–2793. https://doi.org/10.1002/esp.4432

Deutsch, C. V., & Journel, A. G. (1998). *GSLIB geostatistical software library and user's guide*. Oxford University Press.

Fannin, R. J., & Wise, M. P. (2001). An empirical–statistical model for debris-flow travel distance. *Canadian Geotechnical Journal*, *38*(5), 982–994. https://doi.org/10.1139/cgj-38-5-982

Forte, A. M., Brian, J. Y., & Whipple, K. X. (2016). Complexities of landscape evolution during incision through layered stratigraphy with contrasts in rock strength. *41*(12), 1736–1757. https://doi.org/10.1002/esp.3947

Gregoretti, C., & Dalla Fontana, G. (2008). The triggering of debris-flow due to channel-bed failure in some alpine headwater basins of the Dolomites: Analyses of critical runoff. *Hydrological Processes*, *22*(13), 2248–2263. https://doi.org/10.1002/hyp.6821

Gregoretti, C., Degetto, M., Bernard, M., Crucil, G., Pimazzoni, A., De Vido, G., et al. (2016). Runoff of small rocky headwater catchments: Field observations and hydrological modeling. *Water Resources Research*, *52*(10), 8138–8158. https://doi.org/10.1002/2016WR018675

Guadagnini, L., Menafoglio, A., Sanchez-Vila, X., & Guadagnini, A. (2020). Probabilistic assessment of spatial heterogeneity of natural background concentrations in large-scale groundwater bodies through Functional Geostatistics. *Science of the Total Environment*, *740*(2020), 140139. https://doi.org/10.1016/j.scitotenv.2020.140139

Herbert, L., Santi, P., & Densmore, A. (2024). Controls on debris-flow avulsions: White mountains of California and Nevada. *Landslides*, *21*(4), 861–874. https://doi.org/10.1007/s10346-023-02207-3

Höhle, J., & Höhle, M. (2009). Accuracy assessment of digital elevation models by means of robust statistical methods. *ISPRS Journal of Photogrammetry and Remote Sensing*, *64*(4), 398–406. https://doi.org/10.1016/j.isprsjprs.2009.02.003

Hooke, R. L. (1967). Processes on arid-region alluvial fans. *The Journal of Geology*, *75*(4), 438–460. https://doi.org/10.1086/627271

Howard, A. D. (1990). Theoretical model of optimal drainage networks. *Water Resources Research*, *26*(9), 2107–2117. https://doi.org/10.1029/wr026i009p02107

Mallet, C., & Bretar, F. (2009). Full-waveform topographic lidar: State-of-the-Art. *ISPRS Journal of Photogrammetry and Remote Sensing*, *64*, 1–16. https://doi.org/10.1016/j.isprsjprs.2008.09.007

Marchi, L., Dalla Fontana, G., Cavalli, M., & Tagliavini, F. (2008). Rocky headwaters in the Dolomites, Italy: Field observations and topographic analysis. *Artic, Antartic, and Alpine Research*, *40*(4), 685–694. https://doi.org/10.1657/1523-0430(07-037)[marchi]2.0.co;2

Orlandini, S., & Moretti, G. (2009). Determination of surface flow paths from gridded elevation data. *Water Resources Research*, *45*(3). https://doi.org/10.1029/2008WR007099

Pederson, C. A., Santi, P. M., & Pyles, D. R. (2015). Relating the compensational stacking of debris-flow fans to characteristics of their underlying stratigraphy: Implications for geologic hazard assessment and mitigation. *Geomorphology*, *248*, 47–56. https://doi.org/10.1016/j.geomorph.2015.06.030

Rodriguez-Iturbe, I., & Rinaldo, A. (2001). *Fractal River basins: Chance and self-organization*. Cambridge. https://doi.org/10.1063/1.882305

Schiavo, M. (2022). Probabilistic delineation of subsurface connected pathways in alluvial aquifers under geological uncertainty. *Journal of Hydrology*, *615*(22), 128674. https://doi.org/10.1016/j.jhydrol.2022.128674

Schiavo, M. (2023). Entropy, fractality, and thermodynamics of groundwater pathways. *Journal of Hydrology*, *617*(4), 128930. https://doi.org/10.1016/j.jhydrol.2022.1289

Schiavo, M. (2024). Numerical impact of variable volumes of Monte Carlo simulations of heterogeneous conductivity fields in groundwater flow models. *Journal of Hydrology*, *634*, 131072. https://doi.org/10.1016/j.jhydrol.2024.131072

Schiavo, M., Giambastiani, B. M. S., Greggio, N., Colombani, N., & Mastrocicco, M. (2024). Geostatistical assessment of groundwater Arsenic contamination in the Padana plain. *Science of the Total Environment*, *931*, 172998. https://doi.org/10.1016/j.scitotenv.2024.172998

Schiavo, M., Gregoretti, C., Boreggio, M., Barbini, M., & Bernard, M. (2024). Probabilistic identification of debris-flow pathways in mountain fans within a stochastic framework [Dataset and code]. https://doi.org/10.5281/zenodo.13120278

Schiavo, M., Riva, M., Guadagnini, L., Zehe, E., & Guadagnini, A. (2022). Probabilistic identification of preferential groundwater networks. *Journal of Hydrology*, *610*(26), 127906. https://doi.org/10.1016/j.jhydrol.2022.12790

Simoni, A., Bernard, M., Boreggio, M., Lanzoni, S., Stancanelli, L. M., Berti, M., & Gregoretti, C. (2020). Runoff-generated debris-flows: Observation of initiation conditions and erosion-deposition dynamics along the channel at Cancia (eastern Italian Alps). *Earth Surface Processes and Landforms*, *45*(14), 3556–3571. https://doi.org/10.1002/esp.4981

Stahl, S. (2006). The evolution of the normal distribution. *Mathematics Magazine*, *79*(2), 96. https://doi.org/10.2307/27642916

Stoffel, M., Allen, S. K., Ballesteros-Canovas, J. A., & Jacob, M. O. (2024). Climate change effects on debris-flows. In M. Jakob, S. McDougall, & P. M. Santi (Eds.), *Advances in debris-flow science and practice* (pp. 273–308). https://doi.org/10.1007/978-3-031-48691-3

Stoffel, M., Tiranti, D., & Huggel, C. (2014). Climate change impacts on mass movements - Case studies from the European Alps. *Science of the Total Environment*, *493*, 1255–1266. https://doi.org/10.1016/j.scitotenv.2014.02.102

Stroth, A., & McDougall, S. (2021). Societal risk evaluation for landslides: Historical synthesis and proposed tools. *Landslides*, *18*(3), 1071–1085. https://doi.org/10.1007/s10346-020-01547-8

Theule, J. I., Liébault, F., Laigle, D., Loye, A., & Jaboyedoff, M. (2015). Channel scour and fill by debris-flows and bedload transport. *Geomorphology*, *243*, 92–105. https://doi.org/10.1016/j.geomorph.2015.05.003

Thiene, M., Shaw, W. D., & Scarpa, R. (2017). Perceived risks of mountain landslides in Italy: Stated choices for subjective risk reductions. *Landslide*, *14*(3), 1077–1089. https://doi.org/10.1007/s10346-016-0741-3

Tiranti, D., Crema, S., Cavalli, M., & Deangeli, C. (2018). An integrated study to evaluate debris-flow hazard in alpine environment. *Frontiers in Earth Science*, *6*. https://doi.org/10.3389/feart.2018.00060

Tsunetaka, H., Hotta, N., Imaizumi, F., & Hayakawa, Y. S. (2024). Debris-flow fan channel avulsions: An important secondary erosional process along the Ichino-sawa torrent, Japan. *Earth Surface Processes and Landforms*. https://doi.org/10.1002/esp.5994

Van Dijk, M., Kleinhans, M. G., Postma, G., & Kraal, E. (2012). Contrasting morphodynamics in alluvial fans and fan deltas: Effect of the downstream boundary. *Sedimentology*, *59*(7), 2125–2145. https://doi.org/10.1111/j.1365-3091.2012.01337.x

Vosselman, G., & Maas, H.-G. (2010). *Airborne and terrestrial laser scanning* (p. 336). Whittles Publishing.

Wagner, W., Ullrich, A., Ducic, V., Melzer, T., & Studnicka, N. (2006). Gaussian decomposition and calibration of a novel small-footprint full-waveform digitising airborne laser scanner. *ISPRS Journal of Photogrammetry and Remote Sensing*, *60*(2), 100–112. https://doi.org/10.1016/j.isprsjprs.2005.12.001

Yaaqoub, A., & Essaifi, A. (2023). Drainage rearrangement and landscape evolution: Insights from the Moroccan Massif central. *Geomorphology*, *437*, 108811. https://doi.org/10.1016/j.geomorph.2023.108811

Zehe, E., Loritz, R., Edery, Y., & Berkowitz, B. (2021). Preferential pathways for fluid and solutes in heterogeneous groundwater systems: Self-organization, entropy, work. *Hydrology and Earth System Sciences*, *25*(10), 5337–5353. https://doi.org/10.5194/hess-25-5337-2021

Zhou, C., Tan, X., Liu, Y., & Shi, F. (2024). Quantifying the migration rate of drainage divides from high-resolution topographic data. *Earth Surface Dynamics*, *12*(2), 433–448. https://doi.org/10.5194/esurf-12-433-2024

Zubrycky, S., Mitchell, A., McDougall, S., Stroth, A., Clague, J. J., & Menounos, B. (2021). Exploring new methods to analyse spatial impact distributions on debris-flow fans using data from southwestern British Columbia. *Earth Surface Processes and Landforms*, *46*(12), 2395–2413. https://doi.org/10.1002/esp.5184